

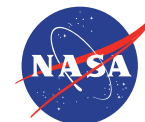


JPL in early April. Artistic rendition of polarized light perception

Depth from Stereo Polarization in Specular Scenes for Urban Robotics

Kai Berger, Randolph Voorhies, Larry H. Matthies

presented at the ICRA 2017 conference
May 29th – June 3rd 2016



Jet Propulsion Laboratory
California Institute of Technology

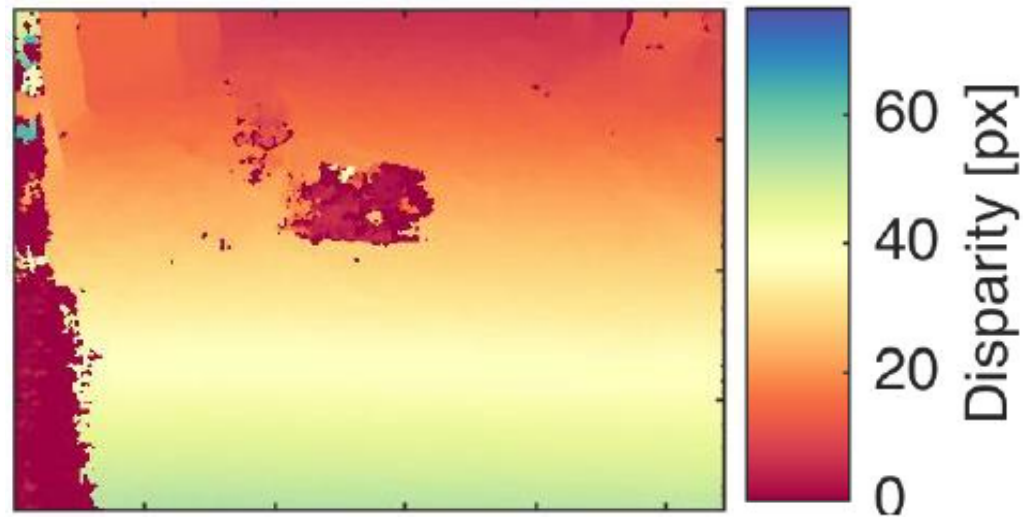
Motivation

- Specular surfaces challenging for typical stereo algorithms in robotics
- SGBM on a water puddle:

R2-water4 (left, 0°)



SGBM



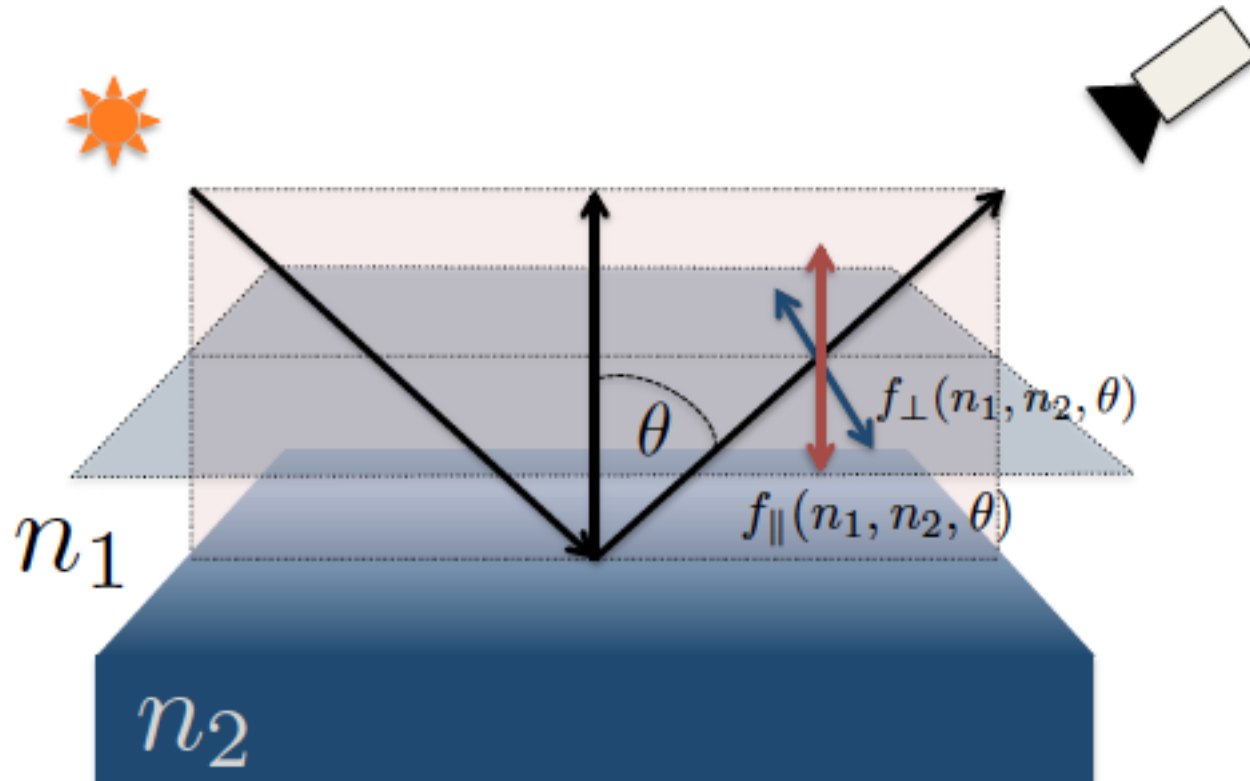
Related Work

For depth perception in specular scenes

- Trinocular and Multicamera Setups [1]
 - Neglect superposition effects
- Time-of flight cameras [2]
 - Limited by range, material, angle of incidence
- Optical Flow [3]
 - Assumptions on Light and surface shape
- Polarization-based [4,5,6]
 - Confined to lab environment
 - Light source known

Light-Surface Interaction

Polarization behavior changes at specular surfaces



Light-Surface Interaction

Polarization behavior changes at specular surfaces



Left view, Polarizer at 0 degrees



Left view, Polarizer at 90 degrees

Light-Surface Interaction

Polarization behavior changes at specular surfaces



Left view, Polarizer at 0 degrees



Left view, Polarizer at 90 degrees

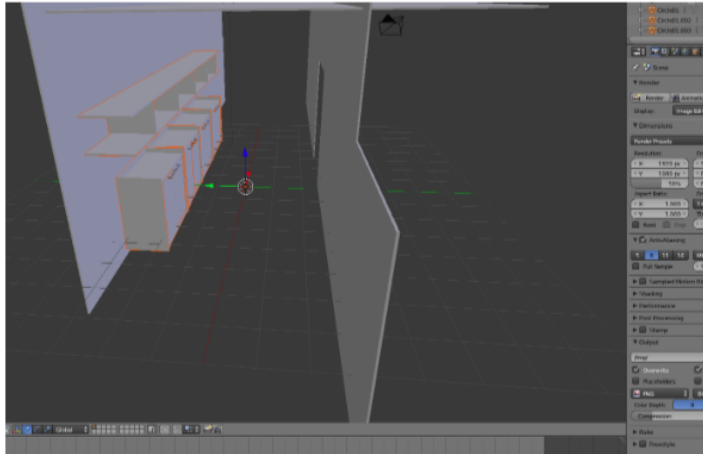
Our Goal: Incorporate polarization into stereo vision

Modus operandi

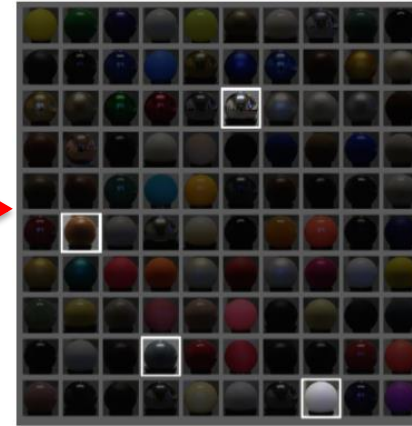
- 1) Provide synthetic data to have ground truth
- 2) Develop and test algorithm on synthetic data
- 3) Capture real-world images with polarizer
- 4) Test algorithm on real-world images

Image Synthesis

1) Model Scene (e.g. with Blender toolkit)

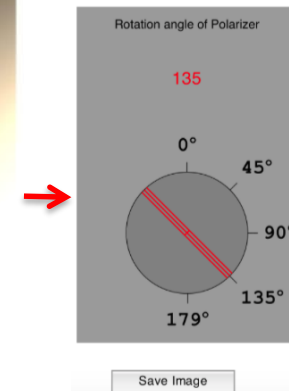
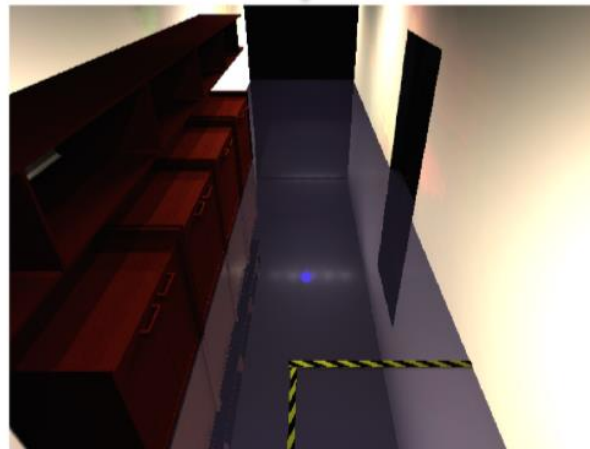


2) Assign material behaviors to surfaces



3) Simulate polarized light transport.
Store Jones Vectors for each pixel.

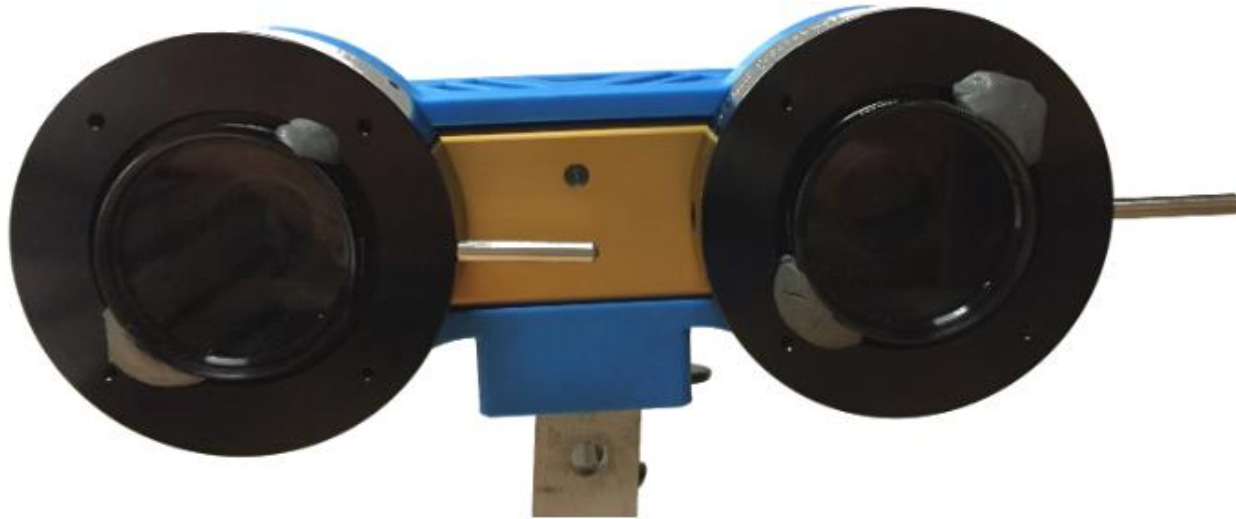
Further, compute stereo images
Store disparity values for each pixel.



4) Display,
virtual linear polarizer

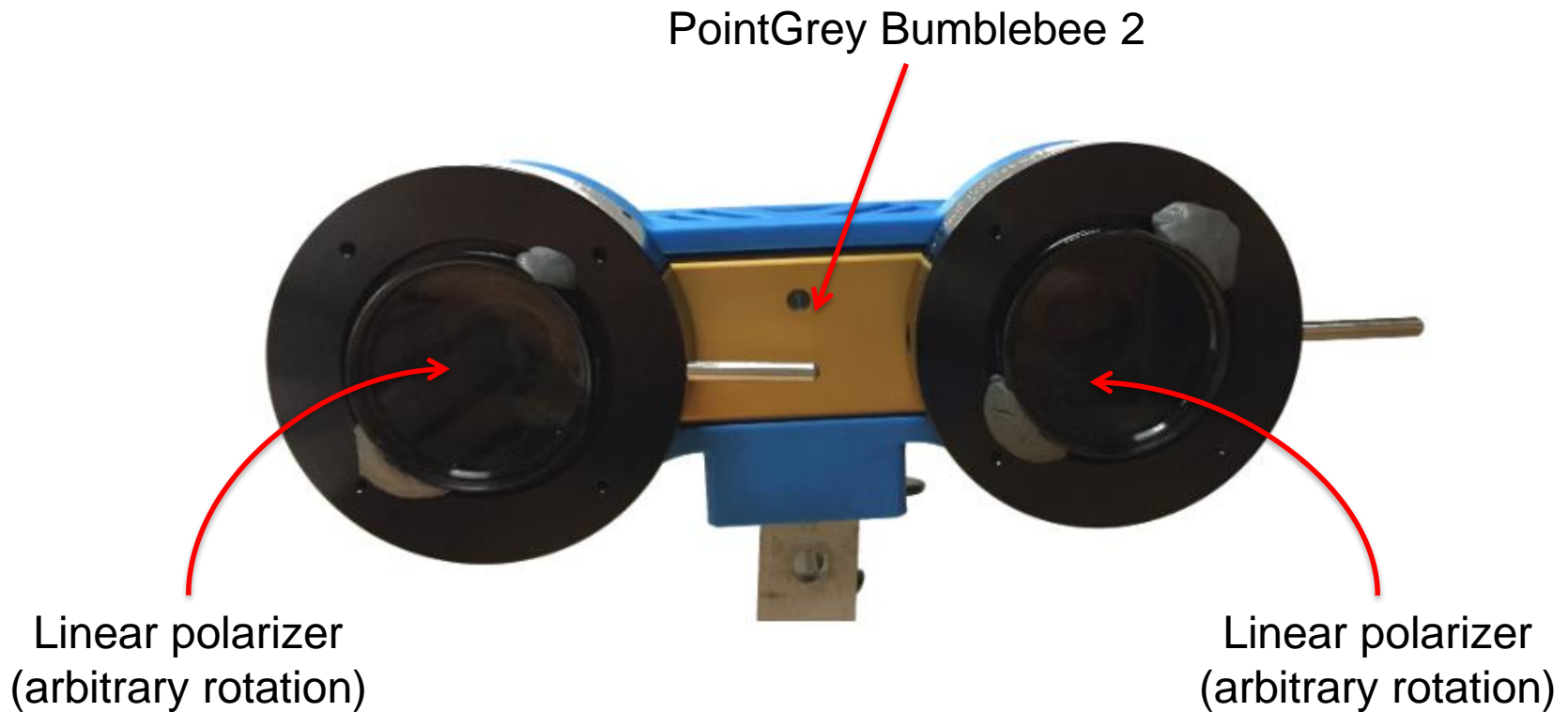
Capturing Setup

Capture 4 images per scene per camera



Capturing Setup

Capture 4 images per scene per camera



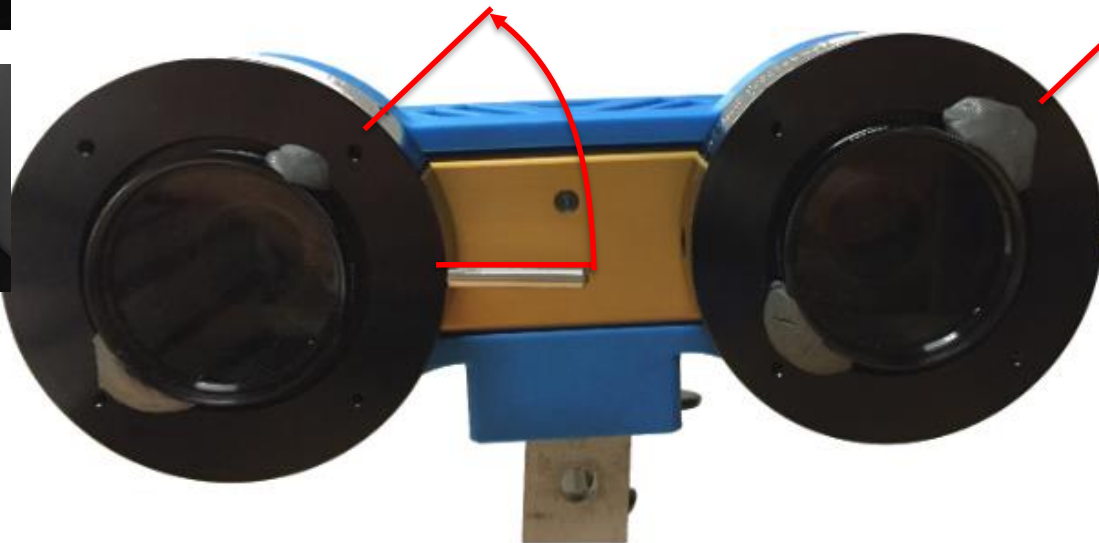
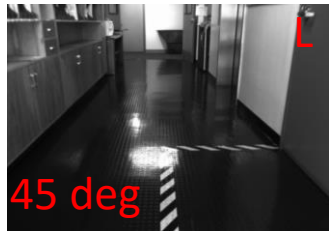
Capturing Setup

Capture 4 images per scene per camera



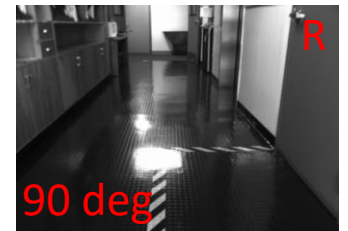
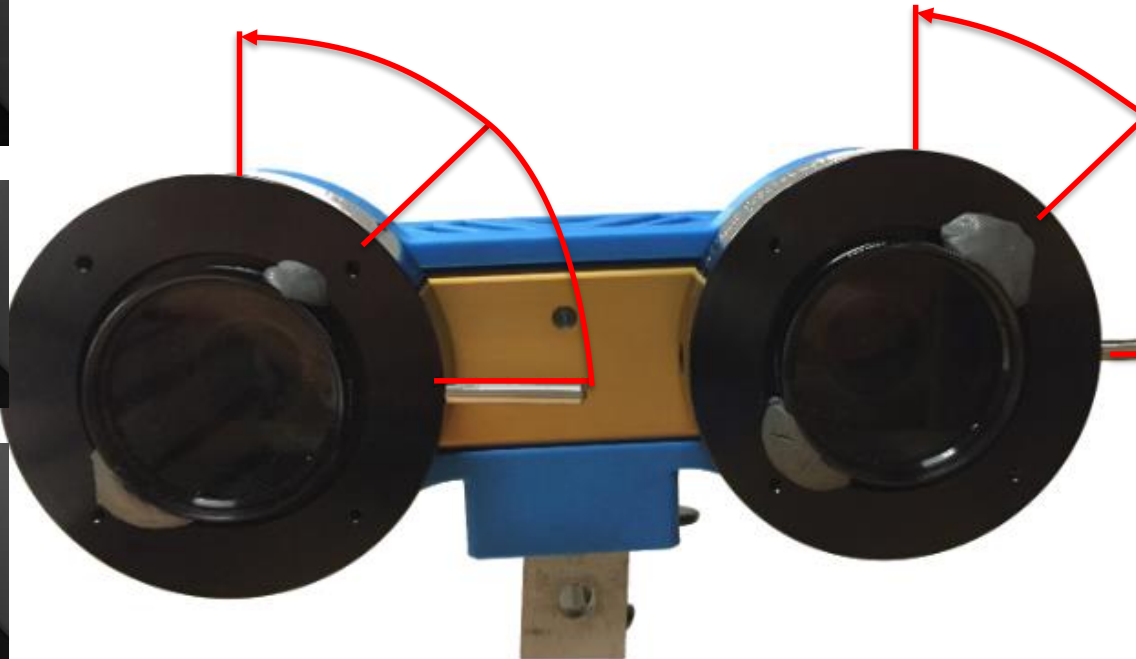
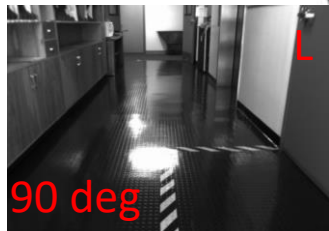
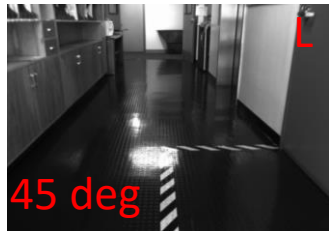
Capturing Setup

Capture 4 images per scene per camera



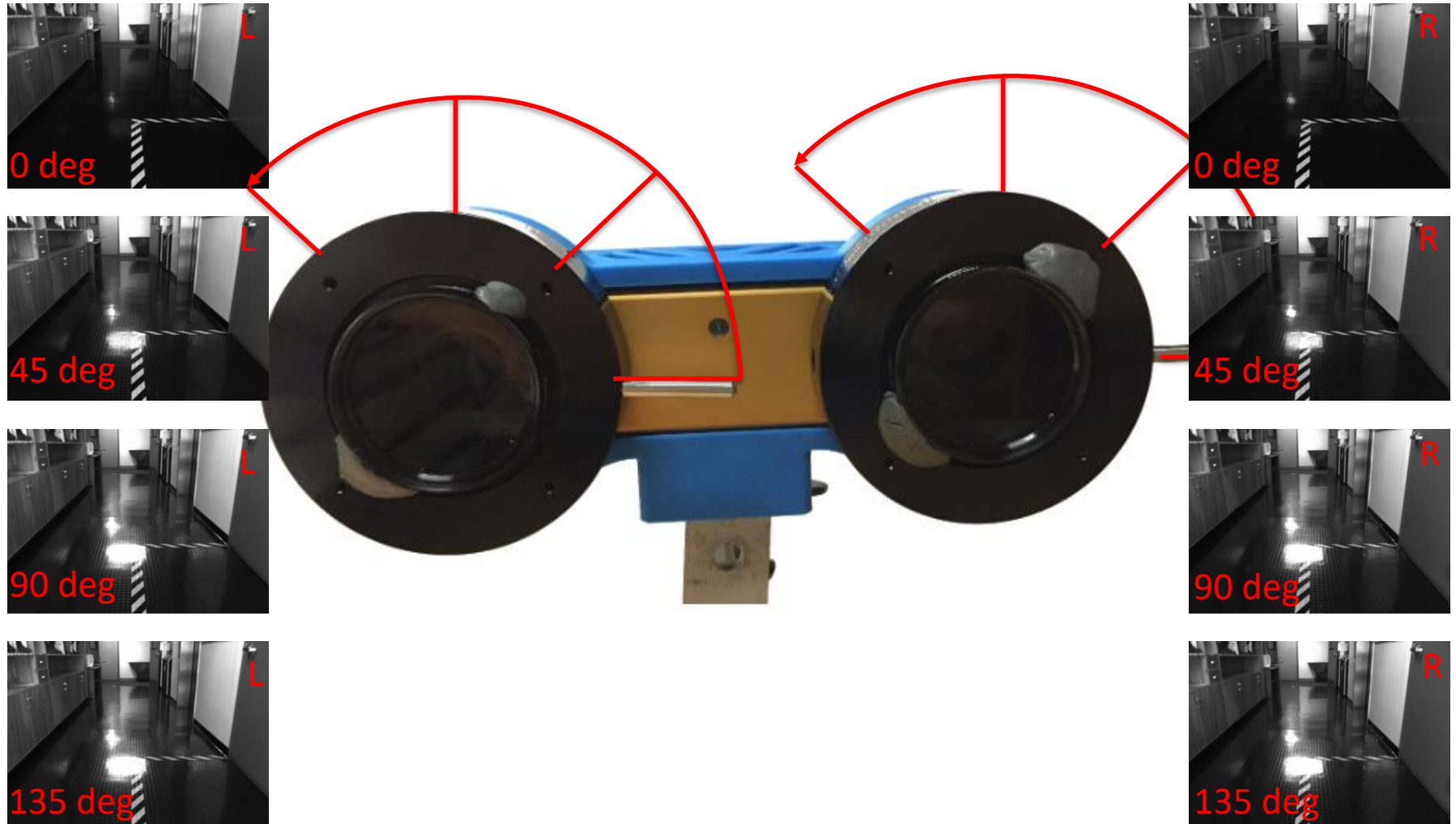
Capturing Setup

Capture 4 images per scene per camera



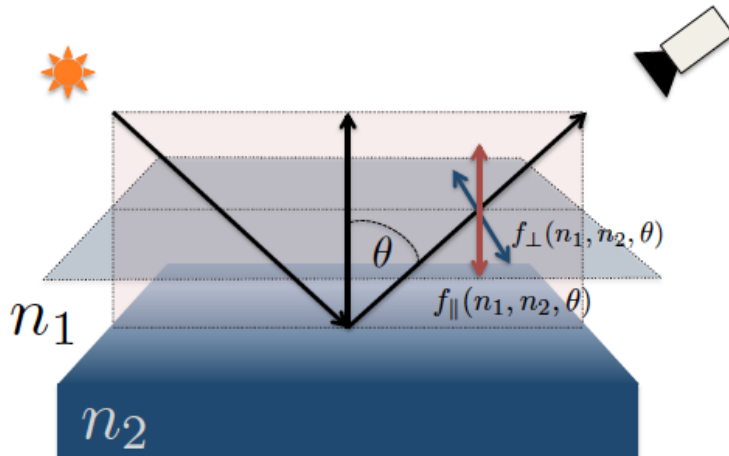
Capturing Setup

Capture 4 images per scene per camera



Graph Cut Approach

- Constrain surface normals by polarization
 - Per pixel Angle of Polarization



$$\text{AOP} = \frac{1}{2} \arctan(S2/S1)$$

with

$$S2 = I_{135} - I_{45}$$

$$S1 = I_{90} - I_0$$

AOP denotes rotation of the plane of incidence around the viewing direction.

This constrains the surface normal to lie in that plane.

Graph Cut Approach

- Constrain surface normals by Polarization
 - Per pixel Angle of Polarization
- Surface smoothness
- Photo-consistency
- Borrow from Woodford et al. [7]

$$\begin{aligned} \min_{D(x)} E_{\text{photo+smooth}} = & \sum_x f(I_1^\Pi(x, D(x)) - I_0(x), V) \\ & + \sum_{\mathcal{N} \in \mathcal{N}} W_1(\mathcal{N}) \rho(\mathcal{S}(\mathcal{N}, \mathcal{D})) \quad (1) \end{aligned}$$

Graph Cut Approach

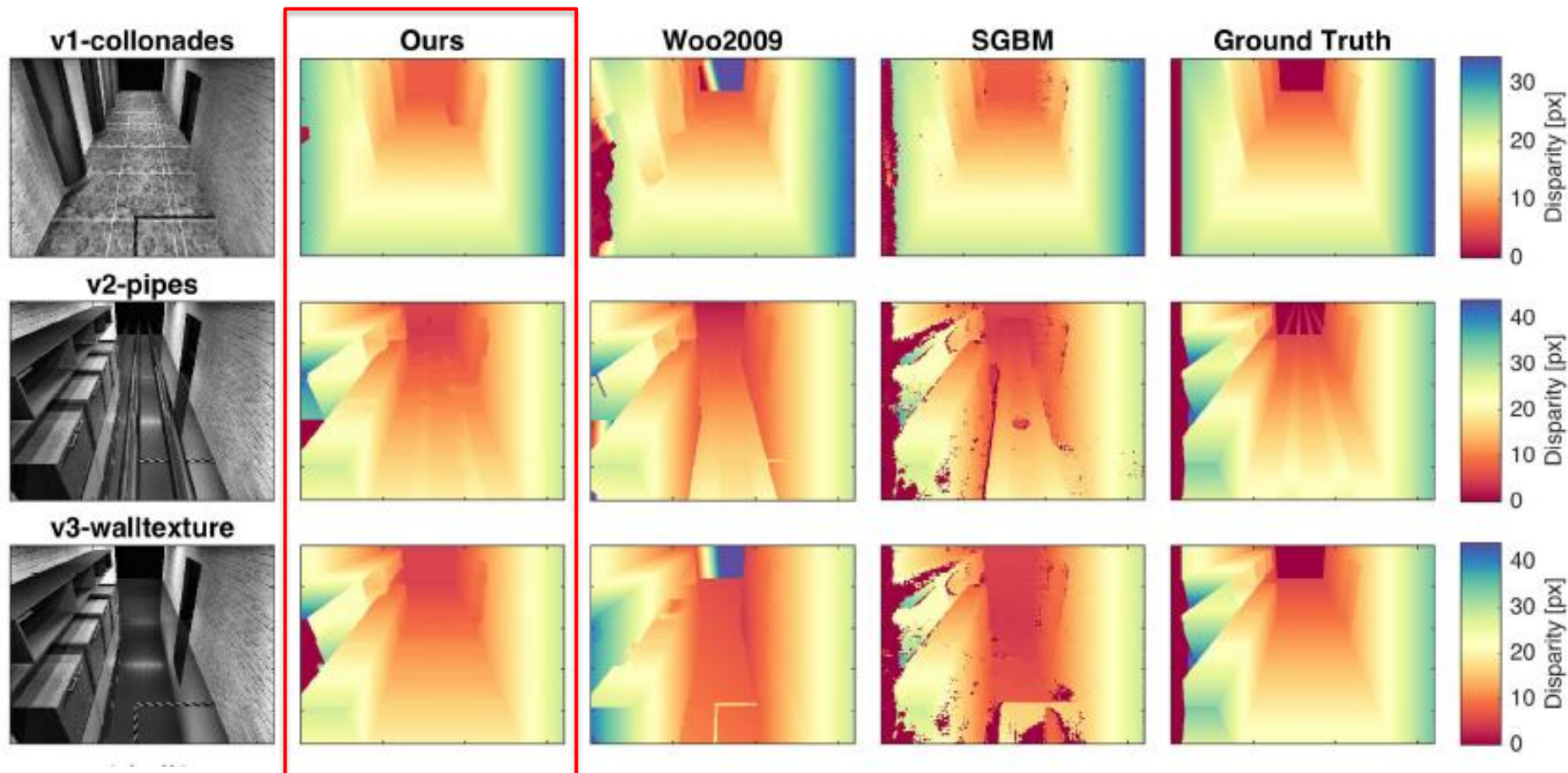
- Add surface normal constraint to [7], arrive at

$$\begin{aligned} E_{\text{photo+smooth}} = & \sum_x f(I_1^\Pi(x, D(x)) - I_0(x), V) \\ & + \sum_{\mathcal{N} \in \mathcal{N}} W_1(\mathcal{N}) \rho(\mathcal{S}(\mathcal{N}, \mathcal{D})) \\ & + \sum_x W_2(\mathcal{N}(x)) \rho(\mathcal{A}(\mathcal{N}(x), \mathcal{D}, \alpha(x))) \end{aligned} \quad (6)$$

$$\begin{aligned} \mathcal{A}(\mathcal{N}, \mathcal{D}, \alpha) = & \tan^{-1}(\Gamma((\Pi^{-1}(p, D(p)) - \Pi^{-1}(q, D(q)) \\ & \times \Pi^{-1}(r, D(r)) - \Pi^{-1}(q, D(q)))) - \alpha), \\ & \{p, q, r\} \in \mathcal{N} \end{aligned} \quad (7)$$

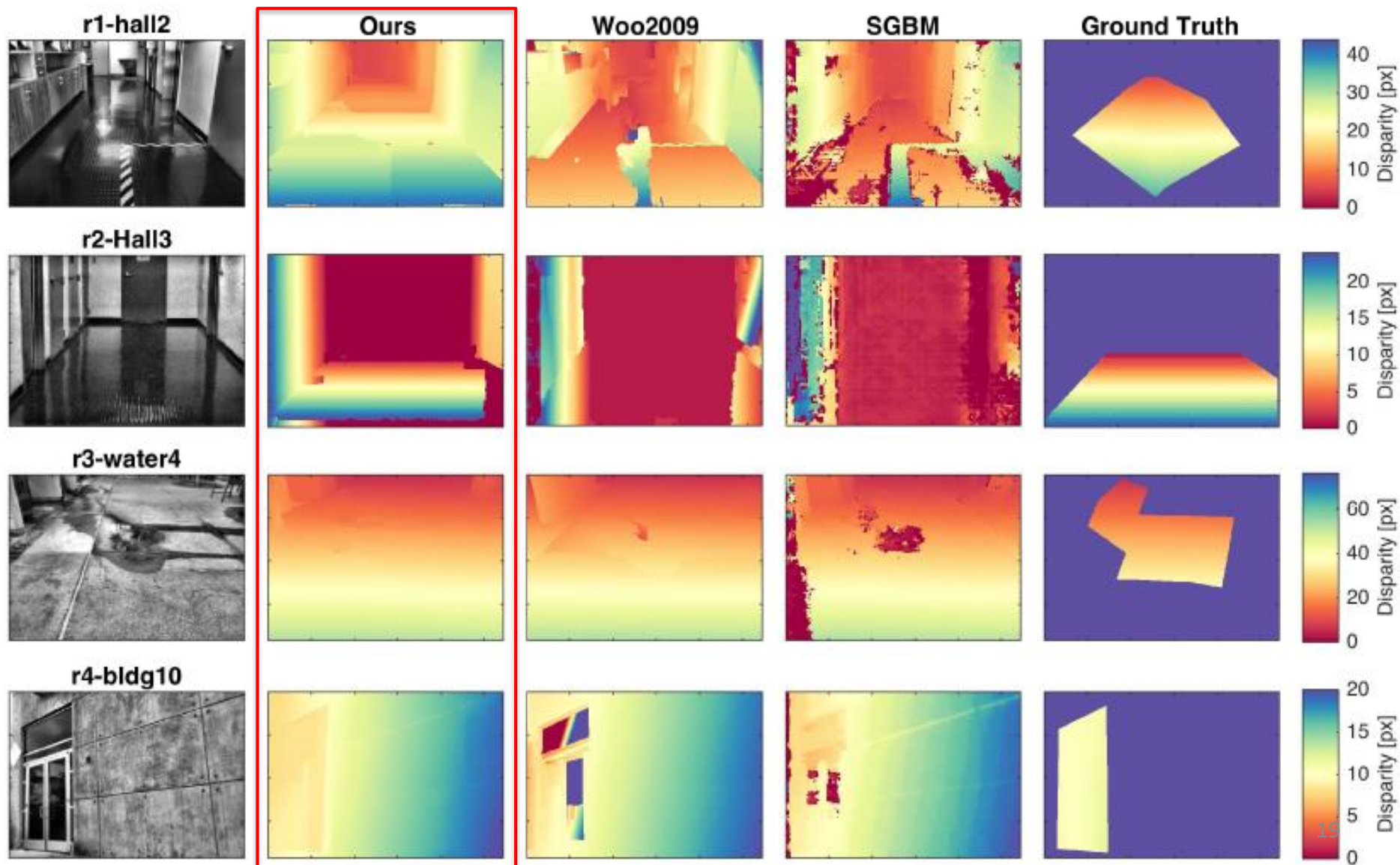
Results

All Scenes (Showing Absolute Difference to Ground Truth)



Results

All Scenes (Showing Absolute Difference to Ground Truth)



Results

All Scenes (Showing Absolute Difference to Ground Truth)

	Ours			Woo2009[25]			SGBM[1]			
	Mean	Out-2 [Percent]	Out-4 [Percent]	Mean	Out-2 [Percent]	Out-4 [Percent]	Mean	Out-2 [Percent]	Out-4 [Percent]	Density [Percent]
v1-collonade	0.608	0.730	0.000	0.651	0.471	0.000	0.545	0.226	0.080	99.755
v2-pipes	0.426	0.424	0.086	1.319	6.206	3.392	1.165	4.913	2.107	98.743
v3-walltexture	0.528	0.041	0.000	4.566	21.012	15.312	5.936	20.938	17.249	98.590
r1-hall2	0.906	3.946	0.038	10.647	25.407	23.605	9.061	21.406	19.023	99.773
r2-hall3	3.713	12.065	5.213	19.435	44.378	40.269	15.771	44.310	40.832	83.598
r3-water4	0.302	0.043	0.000	3.004	4.560	4.287	2.355	3.235	2.823	99.408
r4-bldg10	1.749	7.344	0.000	8.790	7.425	5.433	2.795	13.151	2.369	99.445

Recapitulation

- Specular surfaces and their challenge to stereo vision
- Polarization behavior of reflected light
 - Angle of Polarization
- Simulation of ground truth with Jones calculus
- Real world scenes
 - Multiple images with rotated Linear Polarizers
- Surface normal constraint
 - Applied as ternary term in a graph cut approach
- Improvement over current algorithms in
 - Simulated Scenes
 - Real World Imagery

Fin.

Thank you for your attention.



References

- [1] Bhat, D. N. and Nayar, S. K., *Stereo and specular reflection*, *International Journal of Computer Vision* 26 (2), 91{106 (1998).
- [2] Hebert, M. and Krotkov, E., *3D measurements from image laser radars: how good are they?*, *International Journal of Image and Vision Computing* 10 (3), 170{178 (1992).
- [3] Roth, S. and Black, M. J., *Specular flow and the recovery of surface structure*, in *Conference on Computer Vision and Pattern Recognition*, (2006).
- [4] Wolff, L. B. and Boult, T. E., *Constraining object features using a polarization reflectance model*, *IEEE Transactions on Pattern Analysis and Machine Intelligence* 13 (7), 635{657 (1991).
- [5] Atkinson, G., Hancock, E. R., et al., *Recovery of surface orientation from diuse polarization*, *ImageProcessing*, *IEEE Transactions on* 15 (6), 1653{1664 (2006)
- [6] Kadambi, A., Taamazyan, V., Shi, B., and Raskar, R., *Polarized 3d: High-quality depth sensing with polarization cues*, in *[Proceedings of the IEEE International Conference on Computer Vision]*, 3370{3378 (2015).
- [7] Woodford, O., Torr, P., Reid, I., and Fitzgibbon, A., *Global stereo reconstruction under second-order smoothness priors*, *Pattern Analysis and Machine Intelligence*, *IEEE Transactions on* 31 (12), 2115{2128 (2009).



JPL in early April. Artistic rendition of polarized light perception

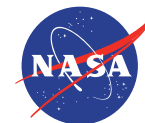
Depth from Stereo Polarization in Specular Scenes for Urban Robotics

Preview Talk

Kai Berger, Randolph Voorhies, Larry H. Matthies

presented at the ICRA 2017 conference

May 29th – June 3rd 2016



Jet Propulsion Laboratory
California Institute of Technology

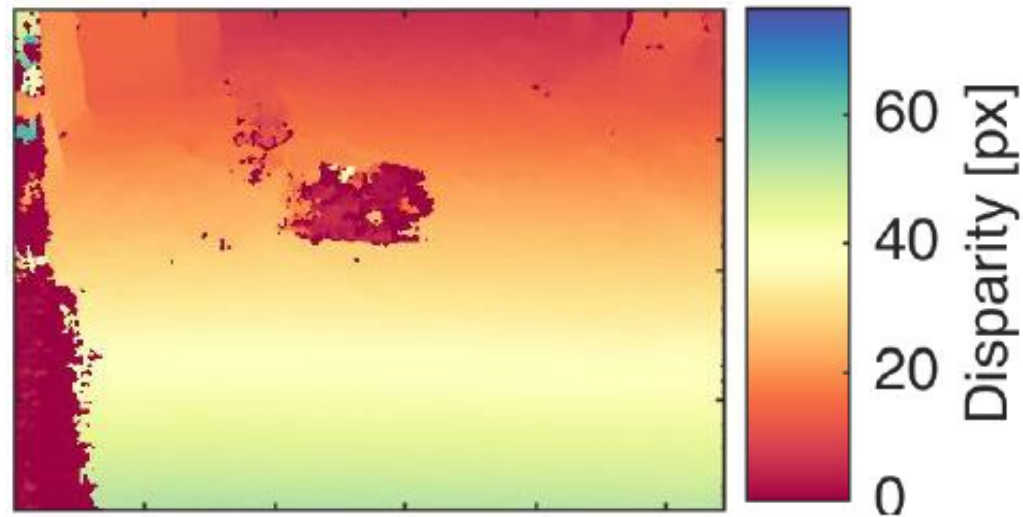
Motivation

- Specular surfaces challenging for typical stereo algorithms in robotics
- SGBM on a water puddle:

R2-water4 (left, 0°)

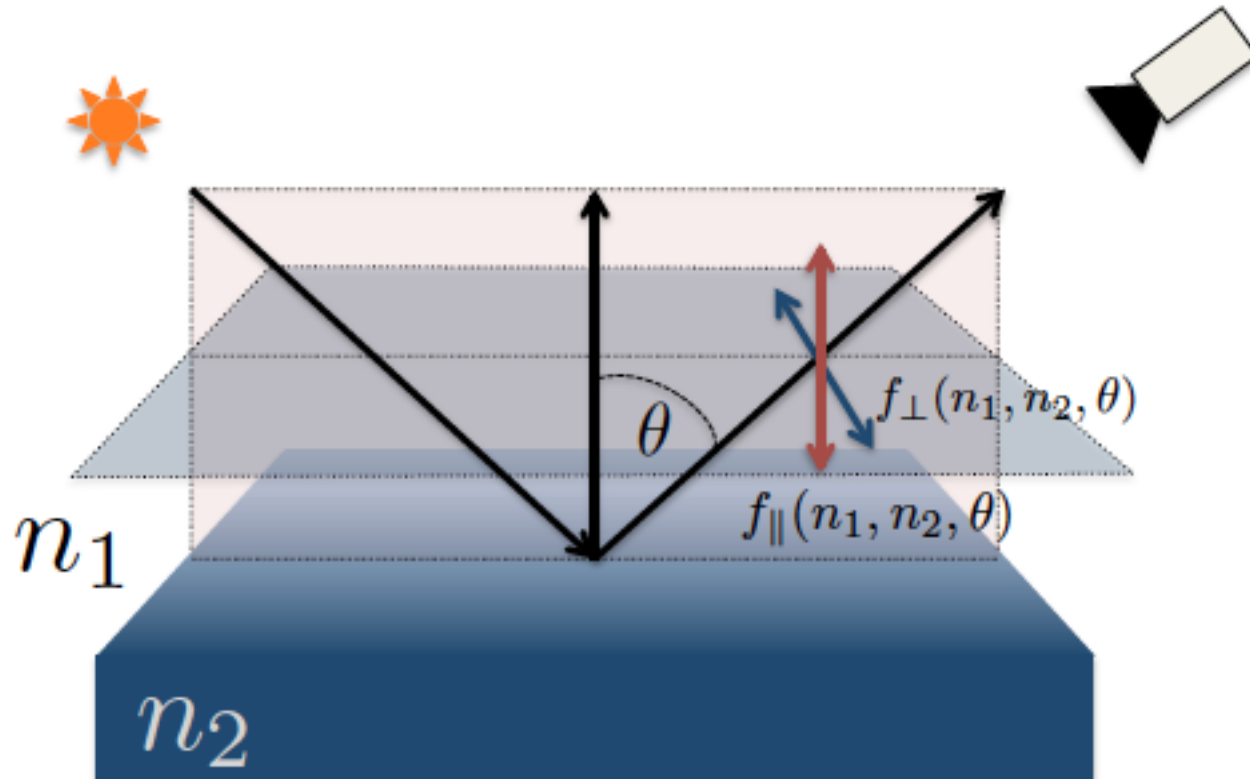


SGBM



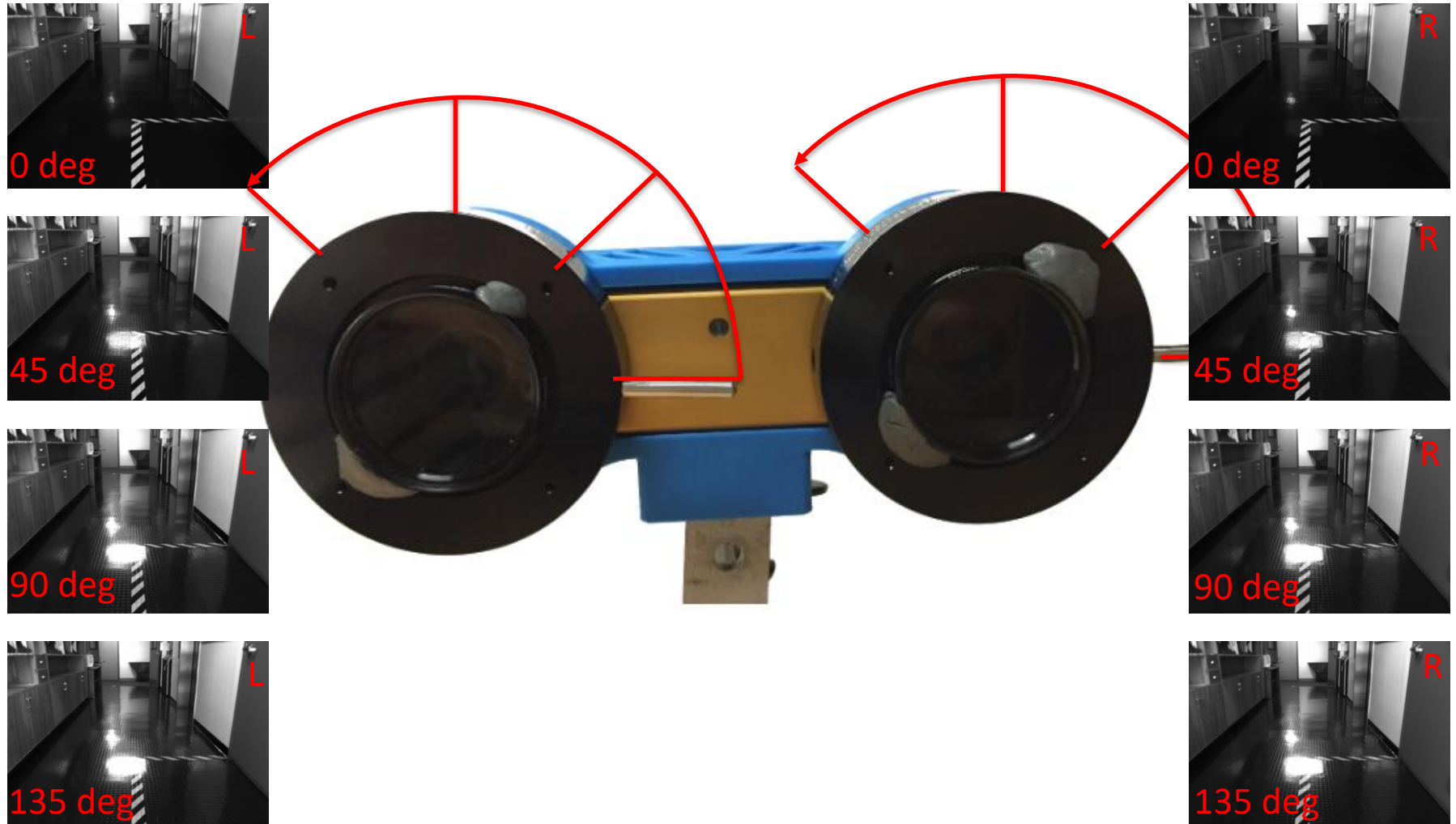
Light-Surface Interaction

Polarization behavior changes at specular surfaces



Capturing Setup

Capture 4 images per scene per camera



Graph Cut Approach

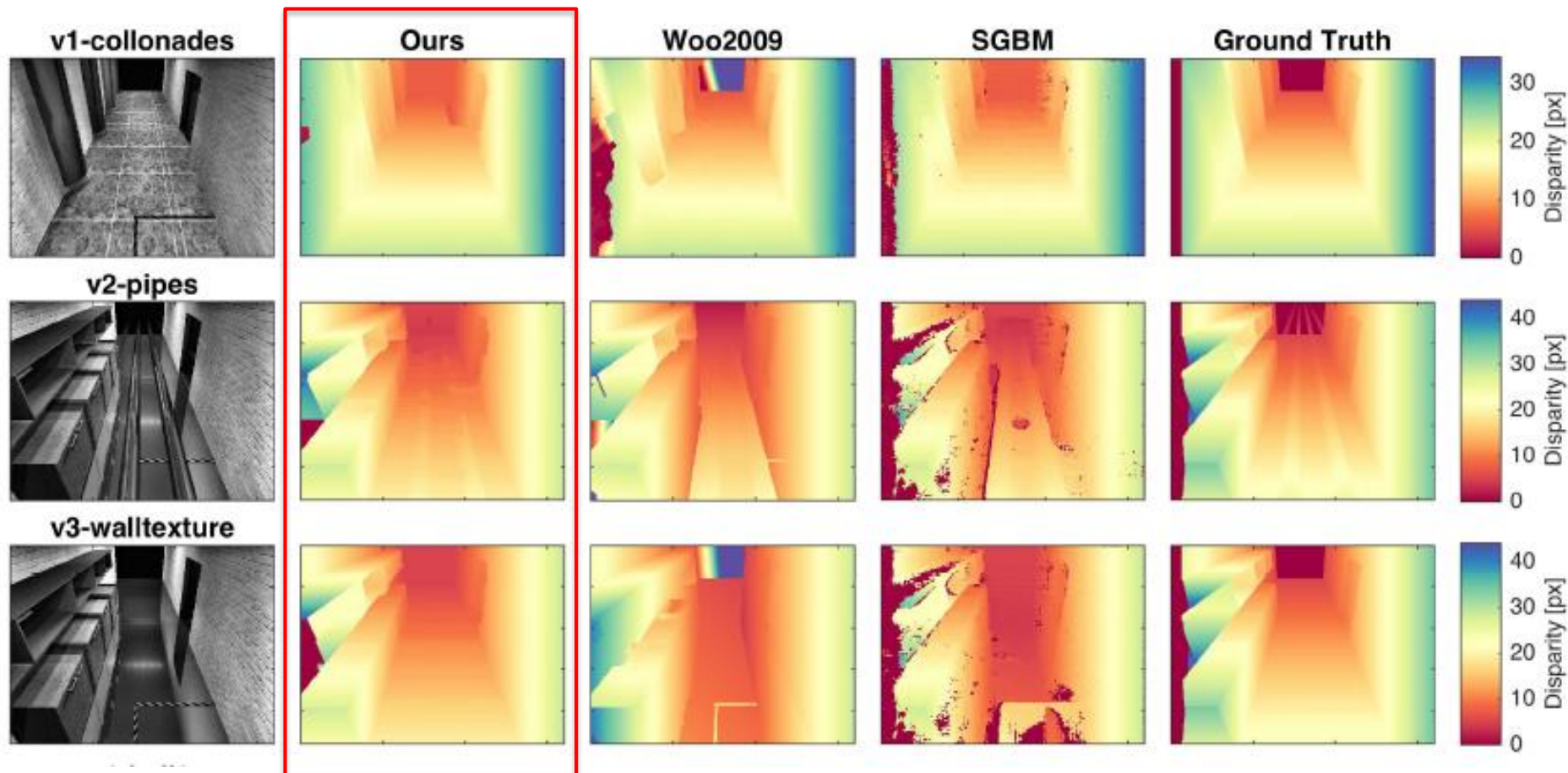
- Add surface normal constraint to [7], arrive at

$$\begin{aligned} E_{\text{photo+smooth}} = & \sum_x f(I_1^\Pi(x, D(x)) - I_0(x), V) \\ & + \sum_{\mathcal{N} \in \mathcal{N}} W_1(\mathcal{N}) \rho(\mathcal{S}(\mathcal{N}, \mathcal{D})) \\ & + \sum_x W_2(\mathcal{N}(x)) \rho(\mathcal{A}(\mathcal{N}(x), \mathcal{D}, \alpha(x))) \end{aligned} \quad (6)$$

$$\begin{aligned} \mathcal{A}(\mathcal{N}, \mathcal{D}, \alpha) = & \tan^{-1}(\Gamma((\Pi^{-1}(p, D(p)) - \Pi^{-1}(q, D(q)) \\ & \times \Pi^{-1}(r, D(r)) - \Pi^{-1}(q, D(q)))) - \alpha), \\ & \{p, q, r\} \in \mathcal{N} \end{aligned} \quad (7)$$

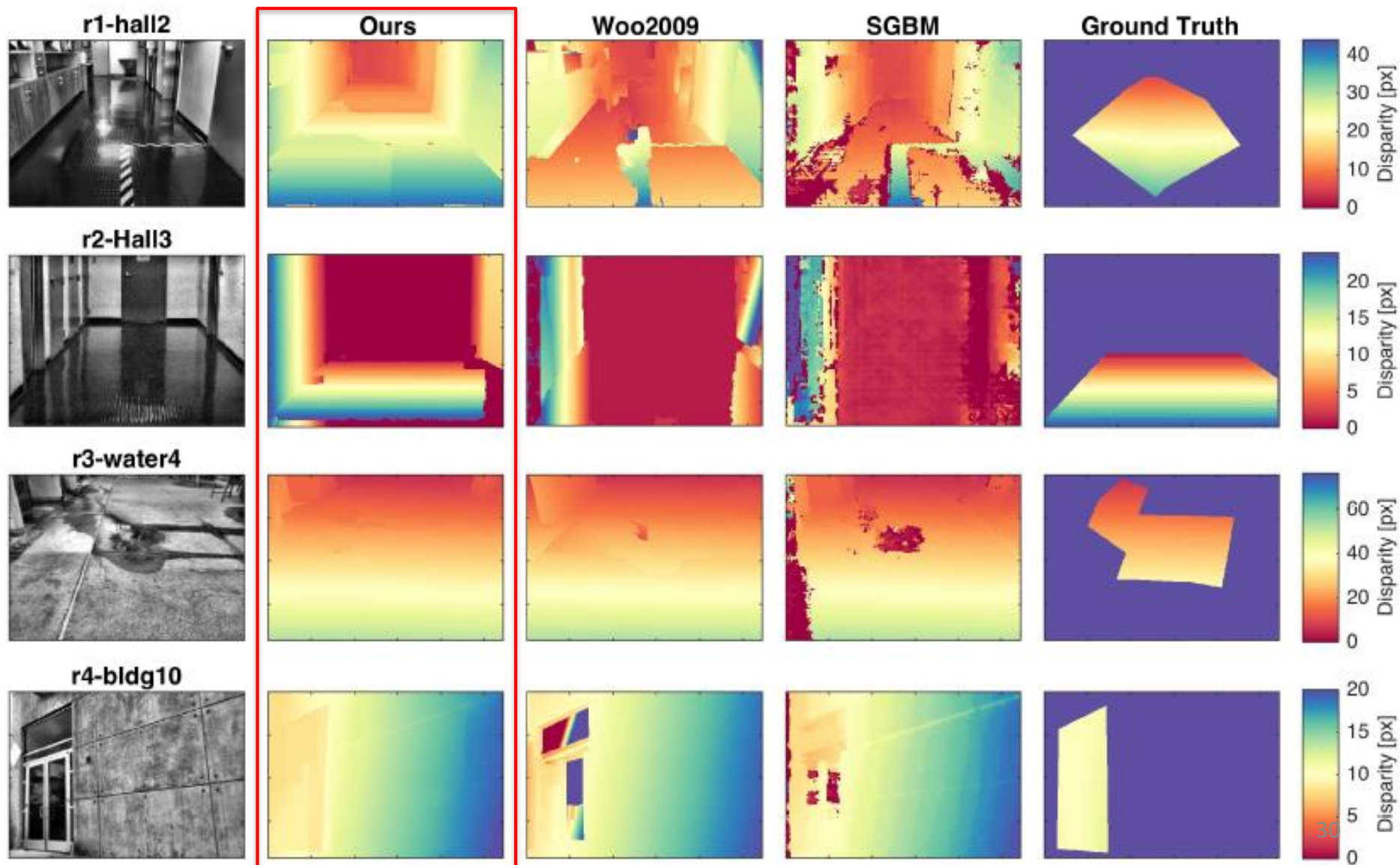
Results

All Scenes (Showing Absolute Difference to Ground Truth)



Results

All Scenes (Showing Absolute Difference to Ground Truth)



Fin.

Thank you for your attention.

